

# Design and Optimization of MIMO Antenna Using Machine Learning Algorithm for IoT Applications

Uruj Jaleel<sup>1</sup>, Mohit Shrivastav<sup>2</sup>

<sup>1</sup>Associate Professor, Department of CS & IT, Kalinga University, Raipur, India.

<sup>2</sup>Research Scholar, Department of CS & IT, Kalinga University, Raipur, India.

## KEYWORDS:

Multiple Input  
Multiple Output,  
Antenna,  
Machine Learning,  
Internet of Things

## ARTICLE HISTORY:

Received 20.09.2024  
Revised 22.10.2024  
Accepted 19.11.2024

## DOI:

<https://doi.org/10.31838/NJAP/06.03.05>

## ABSTRACT

This study presents an innovative dielectric resonance antenna concept for 5G-oriented Internet of Things (IoT) systems within the 6 GHz frequency spectrum sub-band. The antennae are constructed on a 1.5-mm-thickness Flame Retardant Level 4 (FR-4) substrates measuring 35 by 55 mm. The suggested antenna is constructed from alumina and is energized via a 50-ohm microstrip feedline. The combined configuration of circular and rectangle resonance components on the FR4 substrate enhances the radiating process of the proposed device. The antenna layout procedure commences with the creation of the antenna in the Ansys High-Frequency Structure Simulator (HFSS) Electromagnetic (EM) training tool, followed by optimization through machine learning according to the goal parameters of the antenna configuration. A dataset including 2500 samples is constructed in HFSS and utilized by several machine learning methods for optimizing depending on information patterns. Following the optimizing process, the antennae layout is manufactured and evaluated. The suggested antennae provide a broad capacity of 1.2 GHz, from 3.4 to 4.5 GHz, and resonated at 3.8 GHz, rendering it appropriate for 5G IoT scenarios.

**Corresponding Author e-mail:** ku.urujjaleel@kalingauniversity.ac.in, mohit.shrivastav@kalingauniversity.ac.in

**How to cite this article:** Jaleel U, Shrivastav M. Design and Optimization of MIMO Antenna Using Machine Learning Algorithm for IoT Applications. National Journal of Antennas and Propagation, Vol. 6, No. 3, 2024 (pp. 37-42).

## INTRODUCTION

The rapid advancement of wireless techniques and the increasing demand for high-speed communication and connection for Internet of Things (IoT) scenarios have led to the development of innovative antenna layouts.<sup>[1]</sup> Wireless communication technologies have significantly advanced from First-generations (1G) to Fifth-generations (5G) systems.<sup>[2]</sup> Improving reliability, minimizing energy usage, and augmenting channel capacities are crucial for the optimum operation of IoT devices.<sup>[4]</sup> The sub-6 GHz spectrum provides broader coverage, facilitates increased simultaneous relationships, and enhances signal performance for IoT-specific programs in the context of 5G experiences.<sup>[7]</sup> Superior Wide-Band (SWB) technologies are considered the preferred choice in modern wireless communication because of their capacity to produce higher data speeds and improved connection.<sup>[3]</sup> The Federal Communicating Community (FCC) has designated a frequency that spans 3.2-10.5 GHz for application programs, referred

to as the operating bands for Ultra-Wide-Band (UWB) technologies.<sup>[5, 19]</sup>

The deterioration of wide-band antenna structures results from multipath fade. Multipath fading effects can be alleviated by implementing Multiple Inputs Multiple Outputs (MIMO) technologies.<sup>[6]</sup> The MIMO technique utilizes numerous antenna components over a limited area, leading to mutual coupled and subsequent disruptions, alleviating the effects of multiple path fades. The MIMO technique is a communicating method that employs several antennae at both the sending and receiving sides. However, implementing MIMO technologies introduces a further challenge due to reciprocal coupling, characterized by inadequate isolation among adjacent antenna elements. This mutual coupling negatively impacts the system's total effectiveness.<sup>[12]</sup>

Studies utilized multiple ways to tackle this challenge and improve the attained gain, using parasitic decoupling designs, faulty ground infrastructure, slotting stubs, meta substrates, and meta-areas.<sup>[14]</sup> Meta substrates have

numerous possibilities for transmitting technology.<sup>[21]</sup> Changing the radiating structure in the preferred path is necessary to enhance capacity, actual gain, and effectiveness.<sup>[25]</sup> Researchers have employed a meta-substrate communication path to improve the capacity of the antennas [8]. A separate study employed a meta-substrate-based T-matched system to enhance the resistance range.<sup>[20]</sup>

Isolation is a critical element for MIMO setup. Numerous researchers have employed metamaterials and meta-surfaces to enhance significant separation among the components of antennas.<sup>[10]</sup> Isolation augmentation can be achieved using periodical metamaterial-photonic band gaps—numerous studies employed metamaterial electromagnetic bandgap to improve MIMO configurations’ separation between adjacent antenna components.<sup>[11]</sup> Several decoupling designs, including customized U-shaped resonators, enhance isolation.<sup>[18]</sup> In a separate study, the authors used an integrated periphery slot to diminish mutual coupling<sup>[9]</sup>

This study presents the design of a 50 microstrip-feeding stacked (cylinder and rectangle) MIMO antenna. The antenna is modeled using the Ansys High-Frequency Structure Simulator (HFSS) Electromagnetic (EM) training program<sup>[22]</sup> and evaluated using various Machine Learning (ML) methods, including K-nearest neighbors (k-NNs),<sup>[13]</sup> Support Vector Machines (SVMs),<sup>[23]</sup> Random Forests (RFs),<sup>[15]</sup> Decision Trees (DTs),<sup>[16]</sup> Extreme Gradient Boosting (XGB),<sup>[17]</sup> and Linear Regression (LR)<sup>[24]</sup> after being validated by the manufacturer.

**PROPOSED ML-BASED MIMO ANTENNA DESIGN AND OPTIMISATION**

This section outlines the evolution of several geometric characteristics of the suggested antennas. The salient aspects of the antenna creation procedure are also elucidated. The ML algorithms employed to predict the dispersion variables in analyzing the specified design characteristics of the antennas are presented in detail.

**Antenna Geometries**

This sub-area examines the geometrical configuration of the suggested antennas. The proposed design integrates cylinder and rectangle dielectric resonator parts. The dielectric resonance components are positioned near the midpoint of the substrate’s breadth to maximize gain. Flame Retardant Level 4 (FR-4) is the substrate employed for optimal antenna efficiency. A partial surface is placed at the feeding location to provide additional reactance, achieving a wideband response. The di-electrical permeability of FR-4 epoxies is 4.2, with

a substrate width of 1.5 mm. The defective grounding layer mitigates mutual coupling among neighboring dielectric resonances. The microstrip feeding path, measuring 2.5 mm by 21.6 mm, is positioned atop the substrate for coupling purposes. The proposed antennas are placed atop the microstrip path.

A partly ground with dimensions of 13 × 55 mm is applied on the rear side of the FR-4 substrates. To enhance impedance matching, a rectangular slit of 7 mm x 11 mm is carved from the ground surface. The cylindrical dielectric resonator has a radius of 5 mm, a dimension of 9 mm, and a relative permeability of 9.7. The suggested antenna has alumina ceramics. The sizes of the rectangle antenna are 7.5 mm in breadth, 7.5 mm in depth, and 11 mm in height. The disparity in the relative permeability of the dielectric resonances diminishes the efficient dielectric constants. The following equations compute its resonance frequency ( $f_r$ ).

$$f_r = \frac{19 \times 10^7}{2\pi \times D \sqrt{\epsilon_{eff}}} \left\{ 0.29 + 0.35 \left( \frac{D_0}{2 \times H_{eff}} \right) + 0.03 \left( \frac{D_0}{2 \times H_{eff}} \right)^2 \right\} \tag{1}$$

$$H_{eff} = H_0 + H_t \tag{2}$$

$$\epsilon_{eff} = \frac{H_{eff}}{\frac{H_0}{\epsilon_{Al}} + \frac{H_t}{\epsilon_s}} \tag{3}$$

and represent the dimension and elevation of the ceramic substance. and denote the relative permeability and the span of the radiated arrangement, respectively. The resonance frequency, derived from the previously described calculations, is determined to be 3.4 GHz, which closely aligns with the simulated value.

Table 1 illustrates the desired geometric parameters’ rate shift and dimension of steps. It indicates the quantity of specimens generated. The electromagnetic modeling efficiency of the MIMO antennas is achieved using a total of 2500 information points. The scattering variable is expressed in decibels. The supply variables, or independent variables, play a role in antenna layout, whereas the yield factor, or depending parameter, consists of direct values standardized to 50-ohm transmission line impedance data. K-NN, SVM, RF, DT, XGB, and LR techniques are utilized for the objective above.

**Table 1. Database geometrical variable analysis**

Variable	Changing rate	Step dimension	Specimen size
Feeding	20 to 25 mm	0.4 mm	8
Length	5 to 10 mm	1.2 mm	6
Ground	7 to 11 mm	1.2 mm	5
Depth	5 to 8 mm	1.2 mm	6
Width	11 to 16 mm	1.2 mm	5

### Optimization of MIMO Antenna

Figure 1 illustrates the optimizing technique and designing workflow for the suggested MIMO antenna structure. The final optimum model comprises three distinct approaches: achieving necessary efficiency via designing optimization, optimizing the manufactured model’s design efficiency, and selecting design variables to reduce the design area. Choosing design variables involves assessing the relationship between the effectiveness of a specified MIMO antenna pairing. During the layout optimizing procedure in the subsequent phase, databases are produced by EM calculations for every permutation of layout variables, incorporating minor modifications that minimize the number of characteristics.

A deep neural networking (DNN) architecture is suggested to assess every arrangement of design variables, ensuring compatibility for an antenna functioning throughout a broad spectrum of frequency shifts and acquired learning data. This method facilitates the selection of optimal design variables. A MIMO system is constructed utilizing two pairings of MIMO antennas with optimal efficiency, manufactured and generated for testing purposes.

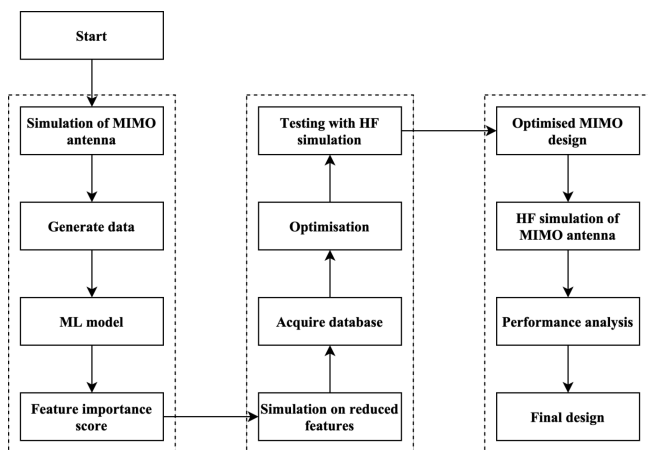


Fig. 1: Workflow of the optimization model

Models and data collecting for the layout validation procedure are conducted using CST MW Studio 2021. The ML algorithms are developed using Tensor-Flow and Python programming with Keras. The complete execution procedure is performed on a system with 8 GB of Random Access Memories(RAM), an i5 processing unit, and a Graphical Processing Unit (GPU). Higher-fidelity models validate designs due to their superior accuracy and increased time usage. Lower-fidelity models are used for data collection due to their time efficiency, albeit with reduced accuracy.

### Validation of gain and effectiveness by ML models

ML approaches have undergone significant research and application in antenna layout over the past decade, owing to their capacity for learning from simulating antenna data via a training process. The measurement result may not precisely reflect its result due to manufacturing mistakes. Regional disparities exist in the accessibility of manufacturing capabilities and measurement instruments. Many studies have employed ML forecasting to corroborate the findings of the antennae. This work validates the achieved gains and effectiveness of the proposed singular-component antennas through ML predictions. A supervised ML method precisely forecasts the antenna’s gain and efficacy.

The execution of ML necessitates two phases. The initial phase involves collecting pertinent data. ML is most effective when utilized with substantial datasets. ML algorithms are subsequently learned on the database to ascertain which yields the most precise forecast. A super wideband antenna is initially developed. The parameterized sweeps are conducted on the dimensions of the antennas’ slots, stubs, surfaces, and feeding lines. These components substantially influence the antenna results. In certain instances, more extensive databases can enhance the performance of ML methods. The impact of a more comprehensive database on a regression system is influenced by various aspects, such as the environmental issue, the size of the input characteristics, and the method’s complexity. Following the collection of 200 data samples through simulation utilizing the CST tool, the subsequent phase entails applying diverse ML methods to estimate the actual gain and effectiveness of the proposed antennas. The database can be partitioned into distinct segments for learning and assessment operations. The technique involves a random database division into learning and evaluation subsets substantiated by statistical proof.

This study utilized forecasts from four separate ML models. Various regression frameworks, such as K-NN, SVM, RF, DT, XGB, and LR, are being evaluated. These methods were chosen due to their efficacy in non-linear evaluation. Regression most effectively executes forecasts because of its emphasis on numerical results. Figure 2 illustrates constructing a database and performing an ML method in flowchart format. The database is prepared and divided into two segments for independent analysis. All ML experiments used Google’s Python modeling and Google Colab application. Initially, partition the database into two halves, designating 75% for training and 25% for testing.

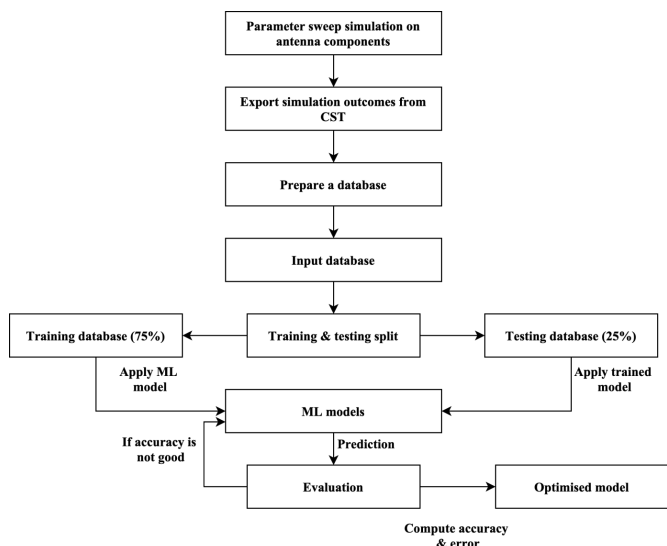


Fig. 2: Workflow of the ML-based training process

RESULTS AND DISCUSSIONS

Experiments are conducted utilizing Ansys HFSS 19.0. The frequency step dimension is set at 0.01 GHz. The highest number of rounds is six; the highest deviation is 0.03. Table 2 displays distinct dimensional specimens of the antennae shape and respective simulations and

ML method outcomes. This data illustrates the gap between the two, serving as evidence of the precision of ML methods.

The proposed algorithm demonstrates superior predictive accuracy when evaluated using the test information compared to all other approaches. The sample size of the information is augmented to achieve significantly more precise findings. The resultant reflecting coefficient,  $\Gamma$ , is -13dB. The capacity measures 1.23 GHz. The operational frequency is 3.47 GHz, spanning from 3.35 to 4.38 GHz.

The accuracy of a regression model for forecasting the targeted parameter can be assessed using various criteria. Evaluating the model across multiple indicators enables efficiency optimization, refinement, and attaining superior results, which is crucial for developing and implementing a generalized approach. Presenting the projected values against the actual figures in the holdout set is the most effective approach to analyzing regression information. The statistical metrics for assessing these frameworks comprise R-squared (R-2), Explaining Variance Scores (Var), Mean Squared Errors (MSEs), Root Mean Squared Errors (RMSEs), Mean Absolution Peak Error (MAPEs), and Mean Absolution

Table 2: Specimen analysis of ML models

Feeding	22.99	23.85	23.75	20.35	22.78	21.76
Length	9.17	5.54	5.07	6.51	7.6	9.76
Depth	6.23	7.72	5.17	7.88	6.97	6.35
Width	15.82	13.06	11.89	11.17	13.1	11.88
HFSS	-18.7	-14.77	-14.12	-15.25	-12.03	-18.39
K-NN	-15.2	-14.87	-17.27	-16.08	-15.59	-16.35
SVM	-16.9	-18.5	-21.29	-19.68	-15.99	-20.54
RF	-14.2	-12.15	-10.15	-12.9	-13.76	-14.43
DT	-18.1	-23.58	-23.42	-19.15	-21.58	-21.82
XGB	-27.1	-26.41	-24.76	-26.6	-22.91	-23.42
LR	-15.9	-20.96	-15.48	-15.87	-15.45	-19.64
Proposed	-13	-12.63	-16.46	-12.66	-12.96	-15.43

Table 3. Gain forecasting analysis

Method	MAE (%)	MSE (%)	RMSE (%)	R-2 (%)	Var (%)	MAPE (%)
K-NN	1.8	3.58	8.8	71.18	73.81	0.51
SVM	8.7	2.65	4.52	67.95	69.68	1.99
RF	2.49	3.97	4.77	89.89	78.94	1.16
DT	2.96	1.48	2.67	88.53	79.07	1.71
XGB	8.36	1.78	13.4	92.44	89.19	0.62
LR	4.81	3.33	6.43	72.33	74.95	1.72
Proposed	0.45	1.17	1.23	57.01	45.33	0.27

Errors (MAEs). Table 3 reviews the relative benefits of different approaches, including K-NN, SVM, RF, DT, XGB, LR, and the proposed system. The precision of each approach is evaluated using many metrics, such as R-2, Var, MSE, RMSE, and MAE.

Figure 3 compares regression methodologies, including K-NN, SVM, RF, DT, XGB, LR, and the proposed system. Multiple metrics, including MAE, MSE, R-2, and Var results, are utilised to analyse the precision of every method. The MAE, MSE, and Var values for the proposed modeling are reported as a minimum. The proposed system attains the maximum R-2 and Var accuracy, corresponding to 64.23% and 63.86%. The median error rate is below 2%. All accessible methods exhibit an accuracy of 97% or above. Given the close resemblance between the training and testing results, the element's gain aligns closely with the simulations.

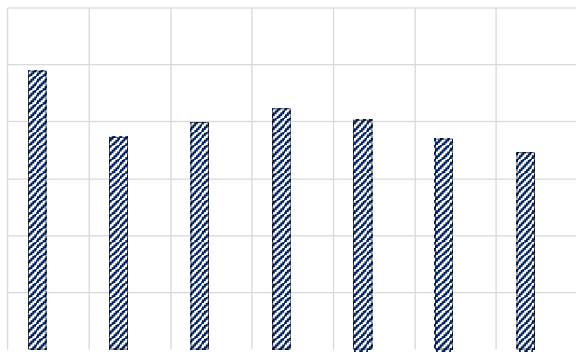


Fig. 3: Accuracy analysis of different ML models at training

Figure 4 delineates the similarities and differences across standard approaches, including K-NN, SVM, RF, DT, XGB, LR, and the proposed system. The LR model has demonstrated moderate errors, with MAE at 4.81, MSE at 3.33, and MAPE at 1.72 across all three parameters. DT exhibited the most significant MSE of all methods evaluated, at 2.96. DT exhibits minimal error when assessed against the MSE standard. The proposed method most reliably predicts the R-2 and Var ratings, respectively, at 69.34% and 68.07%.

Gaussian Process Regressing Model (GPRM) was utilized for every 40 testing specimens in conjunction with the simulation and forecasted effectiveness. The research necessitates a frequency range of 2.5 to 21 GHz, which we have customized to the preference. The representation of the training outcome and the testing result are remarkably similar. Additional models have also achieved accuracy rates of over 95%. The LR approach is the most probable approach to validating effectiveness, and the effectiveness derived from simulation is dependable.

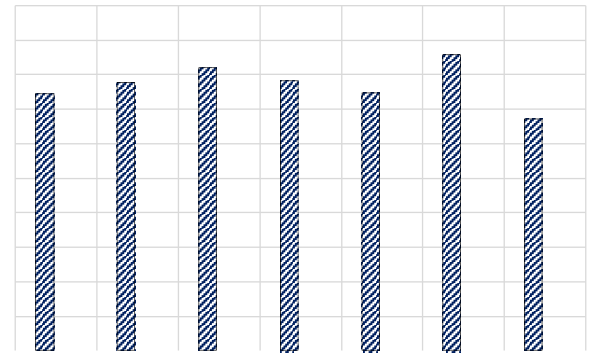


Fig. 4: Accuracy analysis of different ML models at testing

### CONCLUSION

This study involves designing and optimizing MIMO antennas. The suggested antennae are fabricated on an FR-4 substrate with HFSS-simulating tools. The results were subsequently improved according to the efficacy of various ML methods. The proposed technique yields the most suitable and reliable outcomes. The improved antenna has demonstrated favorable radiation effectiveness and total antenna yield outcomes. The engineered antennas possess a capacity of 1.2 GHz and resonate at 3.8 GHz. The suggested antenna provides a broad capacity of 1.2 GHz, from 3.4 to 4.5 GHz, and resonated at 3.8 GHz, rendering it appropriate for 5G IoT scenarios.

### REFERENCES

- [1] Shafique, K., Khawaja, B. A., Sabir, F., Qazi, S., & Mustafaqim, M. (2020). Internet of things (IoT) for next-generation smart systems: A review of current challenges, future trends and prospects for emerging 5G-IoT scenarios. *IEEE Access*, 8, 23022-23040.
- [2] Al-Dujaili, M. J., & Al-dulaimi, M. A. (2023). Fifth-generation telecommunications technologies: Features, architecture, challenges, and solutions. *Wireless Personal Communications*, 128(1), 447-469.
- [3] Balani, W., Sarvagya, M., Ali, T., Samasgikar, A., Das, S., Kumar, P., & Anguera, J. (2021). Design of SWB antenna with triple band notch characteristics for multipurpose wireless applications. *Applied sciences*, 11(2), 711.
- [4] Revathi, S. T., Gayathri, A., Sathya, A., & Santhiya, M. (2023). ECC based Authentication Approach for Secure Communication in IoT Application. *Journal of Internet Services and Information Security*, 13(4), 88-103. <https://doi.org/10.58346/JISIS.2023.14.006>
- [5] Matta, L., Sharma, B., & Sharma, M. (2024). A review on bandwidth enhancement techniques and band-notched characteristics of MIMO-ultra wide band antennas. *Wireless Networks*, 30(3), 1339-1382.

- [6] Ahmad, S., Khan, S., Manzoor, B., Soruri, M., Alibakhshikenari, M., Dalarsson, M., & Falcone, F. (2022). A compact CPW-fed ultra-wideband multi-input-multi-output (MIMO) antenna for wireless communication networks. *IEEE Access*, 10, 25278-25289.
- [7] RANI, MS K. LEELA, et al. "Design and implementation of Triple Frequency Microstrip patch antenna for 5G communications." *International Journal of communication and computer Technologies* 10.1 (2022): 11-17.
- [8] Alibakhshikenari, M., Virdee, B. S., Azpilicueta, L., Naser-Moghadas, M., Akinsolu, M. O., See, C. H., ... & Limiti, E. (2020). A comprehensive survey of "metamaterial transmission-line based antennas: Design, challenges, and applications." *IEEE Access*, 8, 144778-144808.
- [9] Jiménez, D.G., & Le Gall, F. (2015). Testing a Commercial Sensor Platform for Wideband Applications based on the 802.15. 4 standard. *Journal of Wireless Mobile Networks, Ubiquitous Computing, and Dependable Applications*, 6(1), 24-36.
- [10] Kale, R. U., & Sawale, M. D. (2024). A systematic review of design and performance enhancement techniques for the reduction of radar cross section in multiple input multiple output antennas. *Computers and Electrical Engineering*, 120, 109697.
- [11] Nej, S., Ghosh, A., Ahmad, S., Kumar, J., Ghaffar, A., & Hussein, M. I. (2022). Design and characterization of 10-element MIMO antenna with improved isolation and radiation characteristics for mm-Wave 5G applications. *IEEE Access*, 10, 125086-125101.
- [12] Borhan, M. N. (2025). Exploring smart technologies towards applications across industries. *Innovative Reviews in Engineering and Science*, 2(2), 9-16. <https://doi.org/10.31838/INES/02.02.02>
- [13] Geetha, K. (2024). Advanced fault tolerance mechanisms in embedded systems for automotive safety. *Journal of Integrated VLSI, Embedded and Computing Technologies*, 1(1), 6-10. <https://doi.org/10.31838/JIVCT/01.01.02>
- [14] Kumar, TM Sathish. "Low-Power Design Techniques for Internet of Things (IoT) Devices: Current Trends and Future Directions." *Progress in Electronics and Communication Engineering* 1.1 (2024): 19-25.
- [15] Kulkarni, S. S., Sanghai, N. P., Baishya, C., Kumar, A., & Nayak, S. K. (2024). Random forest regression for radiation pattern prediction of planar metasurface reflector antenna. *AEU-International Journal of Electronics and Communications*, 174, 155018.
- [16] Fontoura, L. C., Lins, H. W. D. C., Bertuleza, A. S., D'assunção, A. G., & Neto, A. G. (2021). Synthesis of multiband frequency selective surfaces using machine learning with the decision tree algorithm. *IEEE Access*, 9, 85785-85794.
- [17] Kalayci, H., Ayten, U. E., & Mahouti, P. (2022). Ensemble-based surrogate modeling of microwave antennas using XGBoost algorithm. *International Journal of Numerical Modelling: Electronic Networks, Devices, and Fields*, 35(2), e2950.
- [18] Prasath, C. Arun. "Energy-Efficient Routing Protocols for IoT-Enabled Wireless Sensor Networks." *Journal of Wireless Sensor Networks and IoT* 1.1 (2024): 1-5.
- [19] Sindik, A. (2021). Administrative law and the Federal Communications Commission. *Communication Law and Policy*, 26(3), 312-335.
- [20] Dorofte, M., & Krein, K. (2024). Novel approaches in AI processing systems for their better reliability and function. *International Journal of Communication and Computer Technologies*, 12(2), 21-30. <https://doi.org/10.31838/IJCCTS/12.02.03>
- [21] Kumar, P., Ali, T., & Pai, M. M. (2021). Electromagnetic metamaterials: A new paradigm of antenna design. *IEEE Access*, 9, 18722-18751.
- [22] Anandhi, S., Rajendrakumar, R., Padmapriya, T., Manikanthan, S. V., Jebanazer, J. J., & Rajasekhar, J. (2024). Implementation of VLSI Systems Incorporating Advanced Cryptography Model for FPGA-IoT Application. *Journal of VLSI Circuits and Systems*, 6(2), 107-114. <https://doi.org/10.31838/jvcs/06.02.12>
- [23] Sadulla, S. (2024). Optimization of data aggregation techniques in IoT-based wireless sensor networks. *Journal of Wireless Sensor Networks and IoT*, 1(1), 31-36. <https://doi.org/10.31838/WSNIOT/01.01.05>
- [24] Özkaya, U., Yiğit, E., Seyfi, L., Öztürk, Ş., & Singh, D. (2021). Comparative Regression Analysis for Estimating Resonant Frequency of C-Like Patch Antennas. *Mathematical Problems in Engineering*, 2021(1), 6903925.
- [25] Masoomeh Danesh and Marzieh Emadi. (2014). Cell Phones Social networking software Applications: Factors and Features. *International Academic Journal of Innovative Research*, 1(2), 1-5.
- [26] Du, W. S., Liu, P. T., & Liao, Y. H. (2020). On the mixed reduction: an alternative axiomatization of the fuzzy NTU core. *Results in Nonlinear Analysis*, 3(4), 179-184.